Chemical-wave dynamics in a vertically oscillating fluid layer

G. Fernández-García, D. I. Roncaglia,* V. Pérez-Villar, A. P. Muñuzuri, and V. Pérez-Muñuzuri†
Group of Nonlinear Physics, University of Santiago de Compostela, E-15782 Santiago de Compostela, Spain
(Received 7 May 2007; revised manuscript received 9 October 2007; published 8 February 2008)

Classical Faraday experiments were conducted on the oscillatory chemical Belousov-Zhabotinsky (BZ) reaction. The vertical periodic modulation of the acceleration induces flows in the system that change the BZ dynamics, and thus the patterns exhibited. The resulting reaction-diffusion-advection system exhibits four different types of pattern for increasing stirring amplitude: deformed targets and spiral waves, filamentary patterns arranged in large-scale vortices, advection phase waves, and finally front annihilation where the medium becomes homogeneous. A wave period analysis of the forced system has been carried out. Contrary to what is expected, i.e., a continuous increase of the wave period with increasing forcing, the period changes dramatically at the boundaries between pattern domains.

DOI: 10.1103/PhysRevE.77.026204 PACS number(s): 82.40.Bj, 47.54.−r, 47.70.Fw, 82.40.Ck

I. INTRODUCTION

The formation of spatiotemporal patterns in active media due to the interplay between transport processes and autocatalytic reactions—a ubiquitous phenomenon in nature—is of great relevance to biology, chemistry, etc. [1,2]. In many cases of interest, the reaction-diffusion (RD) dynamics take place in a fluid environment, capable of undergoing a turbulent flow. A host of interesting and little-studied phenomena can be expected from the interplay between mixing and RD dynamics. Their study is important to understanding the dynamics of environmental systems such as plankton populations in the sea [3,4], pollutants in the atmosphere [5,6], and the depletion of the ozone layer [7,8]. A closely related problem that has been numerically studied recently is the role of fluid convection in preexisting RD patterns [9–11]; the formation of patterns in an active medium stirred by chaotic advection has been studied both numerically [12–15] and experimentally [16–18]. Under some circumstances, these flows share the property of displaying coherent structures, i.e., well-defined persisting space-time patterns whose positions and shapes may vary randomly [19–21]. The inhomogeneous distribution of the activating and inhibiting species in the presence of these vortices may drastically change the dynamics of the reaction.

Because of their relevance for natural processes, it is important to identify those cases where the dynamics of active media advected by a flow may be accessible to laboratory experiments. One such case arises when a flow is created through parametric surface excitation. The Faraday experiment—namely, the generation of surface waves on a fluid subjected to purely vertical vibrations—has been extensively studied and has become a model system for pattern formation in hydrodynamic systems [22,23]. In the present work we perform experiments based on the forcing of a Belousov-Zhabotinsky (BZ) reaction [1] by Faraday waves. The resulting reaction-diffusion-advection system exhibits four regions with increasing stirring amplitude: a phase dominated by targets and spiral patterns deformed by the advection flow, filamentary structures organized into vortical structures, synchronized oscillations in the form of reaction-diffusion-advection phase waves, and finally a homogeneous region where no perturbations in the active media were observed.

II. EXPERIMENTAL SETUP

Figure 1 shows a schematic diagram of the experimental setup. Experiments were performed using an electromagnetic shaker (TIRAvib S511, TIRA GmbH) connected to a power amplifier (TIRAvib BAA 120, TIRA GmbH). The shaker supplies a 75 N sine rated peak force, a maximum acceleration of 50g, a maximum rated travel of 10 mm, and a clean frequency range from 2 to 7000 Hz, as specified by the manufacturer. The drive signal for the power amplifier is

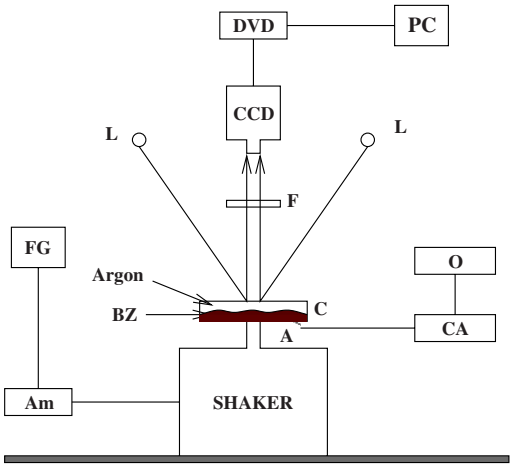

FIG. 1. (Color online) Experimental setup. C is the container, FG the function generator, Am the amplifier, CA the current conditioner, A the accelerometer, O the oscilloscope, F the interference filter 460 nm, PC the personal computer, DVD the digital video device, and L the lamps. Experiments were conducted under an atmosphere of argon.

*Permanent address: Departamento de Ciencia y Tecnología, Universidad Nacional de Quilmes. Saenz Peña 352 (B1876BXD) Bernal, Buenos Aires. Argentina.
†Corresponding author. vicente.perez@cesga.es

obtained from a function generator (HP 33120A). The container's acceleration is measured with a piezoelectric accelerometer (PCB piezotronics M353B18) and a power signal conditioner (PCB piezotronics 480C02), the amplified signal of which is analyzed using a digital oscilloscope (HP 54645A). Therefore acceleration in the vessel container becomes modulated in the form $g=g_0+a\cos(\omega t)$, where g_0 is the gravity force. Experiments were performed in the frequency range $f=\omega/2\pi$ from 7 to 90 Hz for different amplitudes a/g_0.

The reaction takes place in a cylindrical container whose inner diameter is 129 mm. We have used a thin BZ fluid layer of 2 mm height, where the BZ solution is mixed using the following recipe: sulfuric acid 0.9479*M*, malonic acid 0.2604*M*, sodium bromate 0.0594*M*, cerium sulfate 0.0019*M*, and ferroin 0.0008*M*, corresponding to the oscillatory regime. This recipe was chosen because of its large duration and high contrast. The solution is well mixed for 30 min and then dropped into the container. In order to avoid contamination of the surface and minimize evaporation, the cell was closed by a methacrylate cover for visualization of the patterns. Additionally, the inert gas argon is injected in the reservoir to avoid oxygen inhibition in the BZ dynamics [24,25].

The mixture is stirred again inside the container and immediately is recorded from above via a charge-coupled device (CCD) camera and a DVD for postprocessing. The system remains at rest, without patterns, for another 15 min and this time interval is used to measure the bulk oscillation period T_b as well as pattern periods of the unforced system; afterward the shaker is started for 15 min. The value of T_b depends only on the chemical reactants and thus it remained constant during all our experiments. From now on, wave periods shown below will be normalized by this bulk period. The laboratory temperature was held constant at 22 ± 1 °C.

III. RESULTS

A. Faraday behavior

Faraday waves are parametrically excited in the free surface of a fluid when its container is vertically oscillated and the vibration amplitudes exceed some threshold value for a fixed frequency. The frequency of excited waves is usually half the frequency of the vibrated plate at the onset, as first noted by Faraday (subharmonic response) [22]. A harmonic response can also be achieved when the forcing amplitude is increased. Figure 2 summarizes the onset of bifurcations predicted for the Faraday instability (solid lines). These theoretical onset curves were numerically computed following the work of Kumar *et al.* [26,27]. For this purpose, the relevant fluid parameters of the BZ reaction used in the experiments were measured, revealing the following values: density $\rho=1067$ kg/m^3, viscosity $\nu=1.485$ mPa s, and liquid-air surface tension $\sigma=60.9$ mN/m.

In addition to surface waves, a convective flux is induced, as initially noted by Faraday who described a conspicuous accumulation of small particles at the bottom of the vibrated plate. As discussed in the works of Saylor and co-workers [28,29], when the fluid layer is thin, in opposition to their deep layer counterparts, the motion of Faraday waves results in a flow in the fluid region immediately above the bottom, creating oscillatory boundary layers. These velocity fields will play a significant role in the results of our experiments as will be discussed later.

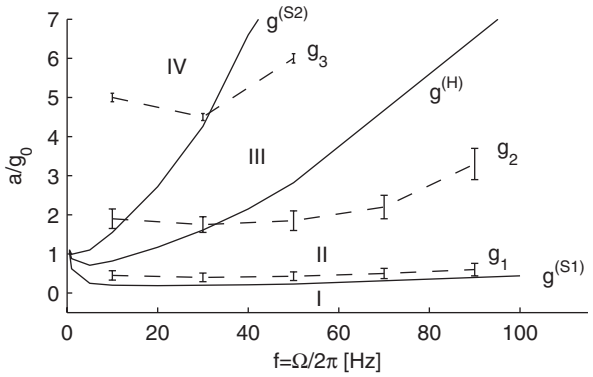

FIG. 2. Phase diagram of BZ Faraday pattern formation as a function of forcing frequency f and acceleration amplitude a/g_0. Continuous lines correspond to the onset of bifurcations predicted for the Faraday instability, where $g^{(S1)}$ indicates the critical amplitude for the first onset of subharmonic waves, $g^{(H)}$ is for harmonic waves, and $g^{(S2)}$ is for the second onset of subharmonic waves. Dashed lines with markers summarize regions with different behaviors observed in the BZ, where g_1 indicates the critical amplitude for the onset of vortically filamentary structures, g_2 is for advection phase waves, and g_3 is for the transition to the homogeneous state. Error bars reflect two facts of important influence in the experiments. On one hand, Faraday patterns are affected by hysteresis. This fact greatly perturbs the critical amplitude g_2 as this amplitude depends on the transition from a concentric ring to stripes or rectangles on Faraday waves. On the other hand, bubbles are generated by the BZ reaction, disturbing both Faraday and BZ waves, especially in regions I and II.

In all of our experiments, the Faraday waves are concentric rings with the same center as the container below the critical amplitude g_2, while stripes or rectangles are the dominant patterns above it.

B. BZ Faraday pattern formation

Figure 2 also summarizes the phase diagram of the experimentally observed BZ patterns (regions I–IV separated by dashed lines). Prior to applying the vibrations, various patterns coexisted in the liquid, including spiral and target waves. These are typical structures usually observed in reaction-diffusion systems. For low acceleration values below the critical amplitude g_1, the active medium is still capable of sustaining patterns equivalent to those observed without forcing, but now appear distorted due to the influence of the fluid flow. In region I the convective velocity flow associated with the Faraday instability is still weak and the reaction behavior is mainly dominated by diffusion.

Above the critical amplitude g_1, region II, the previous BZ patterns are no longer stable in the system and new structures of filamentary type emerge, resulting from the competition between the combined effect of reaction and diffusion with advection [12,16]. Filaments organize forming a well-

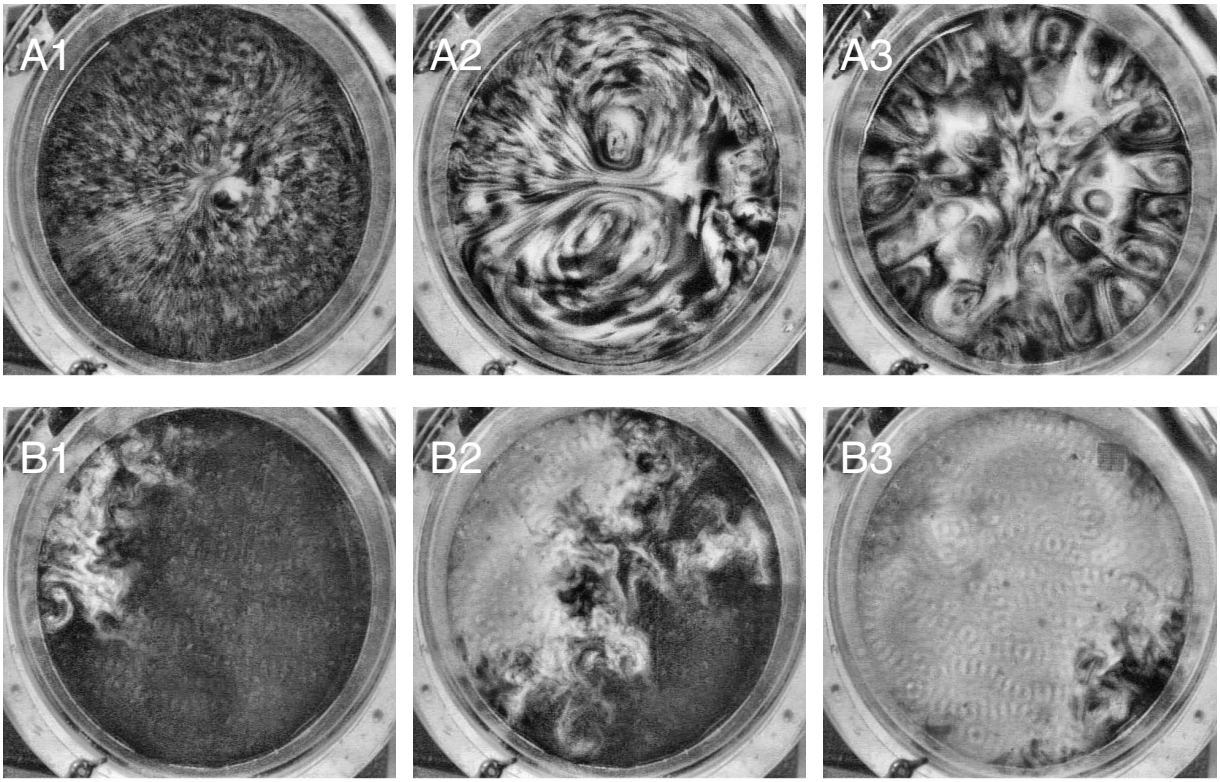

FIG. 3. Experimental patterns observed in the Belousov-Zhabotinsky reaction forced with the Faraday instability. For the upper panels, region II, the forcing frequency is fixed at 7 Hz, while the amplitude a/g_0 changes: 0.6 (A1), 0.8 (A2), and 1.1 (A3), respectively. For the lower panels, region III, as time increases from left to right (7 s between panels), a phase wave ignited at the upper left border spreads over the whole medium ($f=70$ Hz and $a/g_0=2.5$).

defined two-dimensional counter-rotating vortical structure. For low frequencies and amplitudes a small number of vortices may fill the whole domain. From left to right, the upper panels in Fig. 3 show different vortical structures for a fixed forced frequency of 7 Hz as the amplitude is increased. Similar structures were observed for different frequency values. The first panel (A1) shows two small counter-rotating vortices at the center of a radial filamentary structure. As the forcing amplitude is increased, the vortices become larger, filling the whole reactor (A2). For a/g_0 large enough, a ring of vortices near the container border develops (A3), whose width is proportional to the Stokes characteristic length [30]. Increasing (decreasing) the frequency (amplitude) of the forcing leads to a decrease of the ring width. Transients from ordinary active media patterns to filamentary structures when a mixing flow is induced in the medium are well documented in the literature both theoretically [12] and experimentally [16,17].

The whole shape of the filamentary patterns reflects the presence of a large-scale vortex flow in the oscillatory boundary layer. These Faraday-induced vortices were previously reported in [31], where the presence of vortices was attributed to topological defects of Faraday ripples. Mean flows are induced by these defects that are able to entrap and transport passive materials. The vortical structures are also closely related to those in similar experiments consisting of soap films vibrated vertically [32,33].

As the forcing amplitude is increased, a new transition occurs above the critical amplitude g_2. The Faraday waves change their shape from concentric rings to stripes or rectangles.

On the other hand, BZ behavior in this region is dominated by the onset of advection phase waves, i.e., the system becomes homogeneous until periodically a phase wave spreads through the medium. Panels B1–B3 show the depletion of this wave. B1 shows the ignition of the phase wave in the upper-left corner and the spreading of a rough labyrinth interface over the whole system, B2 and B3. Finally the whole system relaxes synchronously until a new perturbation appears. We have also observed that initial perturbations remain in the same region during one experiment, although this region tends to be different from one experiment to another.

For some frequencies and above the critical amplitude g_3, region IV, the medium remains fairly homogeneous during the whole experiment as the mixing strength becomes so large that local perturbations cannot survive, i.e., it is able to keep the whole system homogenized. Note that, for high frequency values, we were not able to reach the critical amplitude g_3 as it is beyond our shaker capabilities.

Once the vibration was turned off, the BZ reaction always recovered normal unforced behavior in all the regions described, i.e., reaction-diffusion patterns (spiral and target waves) reappear in the system after a few minutes. The described behavior is independent of the initial state of the BZ reaction.

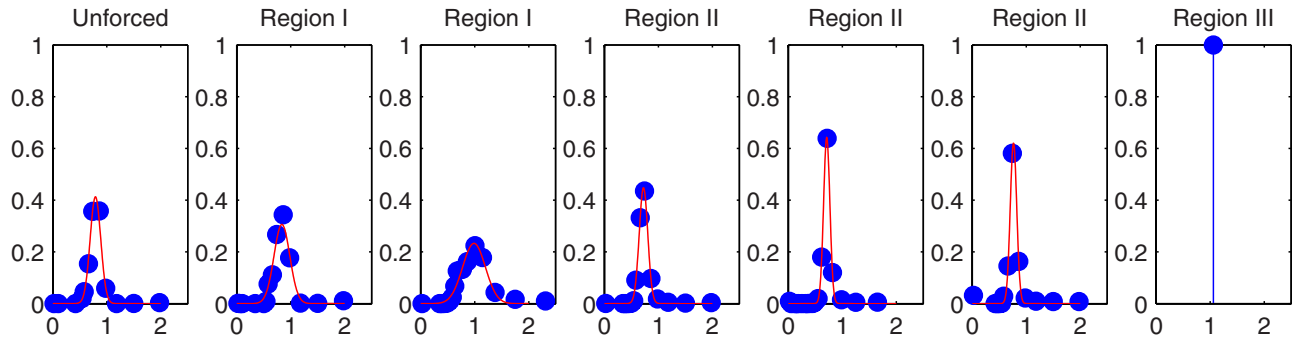

FIG. 4. (Color online) Period distribution for a fixed frequency 30 Hz and increasing amplitudes. From left to right: 0, 0.3, 0.4, 0.7, 1.2, 1.7, and 3.0 in units of g_0. Graphs show the normalized number of occurrences as a function of the normalized wave period T/T_b. For the unforced distributions, periods were measured after 10 min. Labels on top of panels indicate the regions with different behavior observed in the Faraday-BZ system.

C. Period analysis

To gain insight into the experimental results, an analysis of the BZ periods has been carried out. The periods of time between two consecutive waves were measured for each pixel for all recorded frames during the duration of the experiment. Figure 4 shows a typical behavior for the distribution of periods (a periodogram), for increasing acceleration a/g_0. The first panel, from left to right, corresponds to the unforced BZ reaction, where the maximum number of occurrences corresponds to a period smaller than the unforced bulk oscillation period $T/T_b<1$. This is a typical situation as the periods of spiral and target waves are smaller than the phase wave period, which is very close to T_b [34].

The second and third panels in Fig. 4 correspond to acceleration values within region I, i.e., reaction-diffusion structures dominate the BZ reaction. Note that, as advection increases, the peaks become wider and the maximum value shifts toward the unforced bulk oscillation period T_b. The previous patterns, spiral and target waves, have been mixed up, and only the wave portions survive whose period approaches the unforced bulk one. In region II, the fourth through the sixth panels in Fig. 4, vortical structures have replaced diffusion-dominated patterns. Once filaments develop, the period distribution is displaced to lower values than for the diffusion-dominated patterns. The peaks also become narrower, and the period corresponding to the maximum of the spectrum is smaller than the unforced bulk oscillation period. Increasing the forcing acceleration also shifts the dominant frequency peak of the spectrum toward T_b. Finally, the last panel corresponds to region III, where only advection phase waves are observed, whose period equals the unforced bulk oscillation period.

Figures 5(a) and 5(b) summarize the observed behaviors for increasing forcing amplitudes and frequencies, respectively. In Fig. 5(a), the period corresponding to the maximum of the distribution, Fig. 4, is plotted against a/g_0. Note that regions I–III are clearly visible. For region II, close to the boundary with region I, the maximum period is shifted toward smaller values due to filament formation. These smaller periods are in agreement with the size of the filamentary structures, which are thinner and fill the medium densely for smaller values of a/g_0. However, the periods in region III almost remain constant, i.e., the advection phase waves have the same period as the bulk oscillation period T_b. Finally, for Fig. 5(b), the frequency increases while a/g_0 is kept constant and, although the results are not conclusive, the wave periods seem to decrease, at least for large frequency values. Similar behaviors to the ones shown in Figs. 5(a) and 5(b) were obtained for different values of the forcing.

IV. DISCUSSION AND CONCLUSIONS

We have observed experimentally the onset of four regimes as the forcing amplitude in a vertically vibrated active medium increases. The patterns adopt different shapes and behavior as they adapt to forcing. Reaction-diffusion patterns

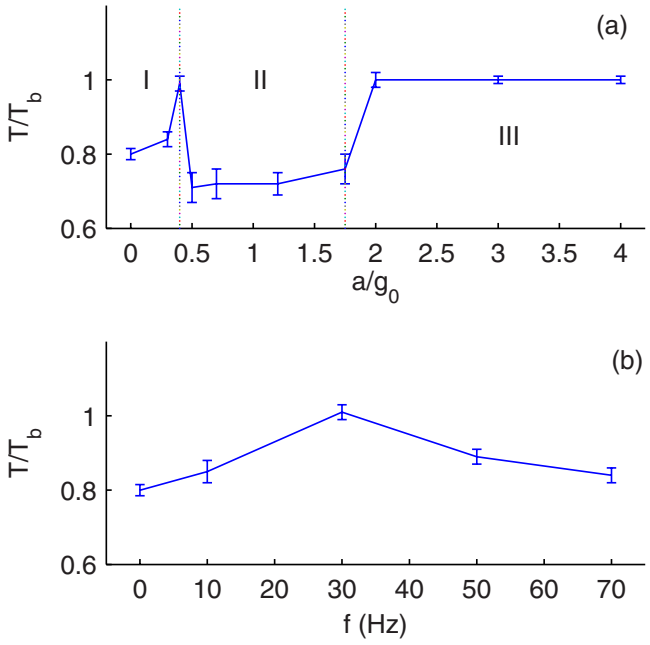

FIG. 5. (Color online) Mean normalized wave period corresponding to the maximum spectrum of Fig. 4 as a function of the forcing amplitude for constant frequency $f=30$ Hz in (a) and as a function of the forcing frequency for constant $a/g_0=0.4$ in (b). (b) lies in region I. Dashed lines in (a) coincide with critical amplitudes g_1 and g_2 separating regions I–III.

have been observed in the unforced medium. For small values of the external forcing they are able to persist but are distorted by advection; the mean period increases and the wave fronts deform. As the forcing increases, the diffusion patterns are no longer stable and new patterns dominated by advection emerge. Filamentary patterns organize themselves reflecting the underlying flow; a large-scale two-dimensional counter-rotating vortical structure. When external forcing is again increased, a transition occurs in the Faraday waves in their shape, strength, and induced convection. The previous patterns are no longer stable in this scenario and the only coherent structures in the active medium are phase waves whose period, as for the unforced system, is very close to the bulk oscillation period.

The periods have been measured for each experiment, obtaining a global increase for increasing acceleration a/g_0 within regions I and II. In region III (advection phase waves) the period remains constant and equal to the bulk oscillation period. A wave period increase due to the presence of advection (as for regions I and II) has been previously reported in [15] for the case of excitable media. In this case, for a critical forcing amplitude, the wave period reaches a maximum value and starts decreasing as patterns become almost absent. In our experiments, a similar behavior was obtained: the period increases for $a/g_0 < g_1$ and it rapidly decreases afterward, when filamentary patterns replace targets and spiral waves. The main difference from the numerical model proposed in [15] is the maximum period obtained, which for our case is the bulk oscillation period. Here, further increasing the forcing amplitude leads to a new period increase; the period becomes constant and equal to T_b for $g_2 < a/g_0 < g_3$. For $a/g_0 > g_3$, region IV, any excitation is annihilated and the fluid is homogeneously mixed.

The purpose of this paper was to investigate the role of the convective flows generated by Faraday waves in BZ chemical patterns. This was achieved with the experimental setup described above. However, although beyond the scope of this paper, further experiments should be performed taking into account the layer depth, the cell diameter, and the surface tension at the fluid surface, among other factors. In addition, the role of different Faraday patterns (chaos, etc.) in BZ dynamics should also be considered.

ACKNOWLEDGMENTS

The authors thank I. Berenstein, A. Garcimartín, and E. Hernández-García for helpful discussions. This work was supported by Ministerio de Educación y Ciencia and Xunta de Galicia under Research Grants No. FIS2007-64698 and No. PGIDIT07PXIB-206077PR, respectively.

[1] *Chemical Waves and Patterns*, edited by R. Kapral and K. Showalter (Kluwer Academic, Dordrecht, 1993).
[2] M. C. Cross and P. C. Hohenberg, Rev. Mod. Phys. **65**, 851 (1993).
[3] E. R. Abraham, Nature (London) **391**, 577 (1998).
[4] E. R. Abraham *et al.*, Nature (London) **407**, 727 (2000).
[5] A. Wonhas and J. C. Vassilicos, Phys. Rev. E **65**, 051111 (2002).
[6] D. Poppe and H. Lustfeld, J. Geophys. Res. **101**, 14373 (1996).
[7] S. Edouard *et al.*, Nature (London) **384**, 444 (1996).
[8] O. Paireau and P. Tabeling, Phys. Rev. E **56**, 2287 (1997).
[9] V. N. Biktashev, A. V. Holden, M. A. Tsyganov, J. Brindley, and N. A. Hill, Phys. Rev. Lett. **81**, 2815 (1998).
[10] J. I. Ramos, Chaos, Solitons Fractals **12**, 1897 (2001).
[11] V. Pérez-Villar, A. P. Munuzuri, M. N. Lorenzo, and V. Perez-Munuzuri, Phys. Rev. E **66**, 036309 (2002).
[12] Z. Neufeld, Phys. Rev. Lett. **87**, 108301 (2001).
[13] I. Z. Kiss, J. H. Merkin, and Z. Neufeld, Phys. Rev. E **70**, 026216 (2004).
[14] V. Pérez-Muñuzuri, Phys. Rev. E **73**, 066213 (2006).
[15] V. Pérez-Muñuzuri and G. Fernández-García, Phys. Rev. E **75**, 046209 (2007).
[16] C. R. Nugent, W. M. Quarles, and T. H. Solomon, Phys. Rev. Lett. **93**, 218301 (2004).
[17] M. S. Paoletti, C. R. Nugent, and T. H. Solomon, Phys. Rev. Lett. **96**, 124101 (2006).
[18] V. Pérez-Villar, J. L. F. Porteiro, and A. P. Munuzuri, Phys. Rev. E **74**, 046203 (2006).
[19] J. M. Ottino, *The Kinematics of Mixing* (Cambridge University Press, Cambridge, U.K., 1989).
[20] J. M. Ottino, Chaos **12**, 400 (2002), special issue on activity in chaotic flows.
[21] T. Tél *et al.*, Phys. Rep. **413**, 91 (2005).
[22] M. Faraday, Philos. Trans. R. Soc. London **121**, 319 (1831).
[23] J. W. Miles and D. Henderson, Annu. Rev. Fluid Mech. **22**, 143 (1990).
[24] O. Steinbock *et al.*, J. Phys. Chem. A **104**, 6411 (2000).
[25] Y. Y. Kalishyn *et al.*, Phys. Chem. Chem. Phys. **7**, 1680 (2005).
[26] K. Kumar and L. Tuckerman, J. Fluid Mech. **279**, 49 (1994).
[27] K. Kumar, Proc. R. Soc. London, Ser. A **452**, 1113 (1996).
[28] P. H. Wright and J. R. Saylor, Rev. Sci. Instrum. **74**, 4063 (2003).
[29] J. R. Saylor and A. L. Kinard, Phys. Fluids **17**, 047106 (2005).
[30] P. K. Kundu, *Fluid Mechanics* (Academic Press, New York, 1989).
[31] A. B. Ezersky, S. V. Kiyashko, and A. V. Nazarrovky, in Control of Oscillations and Chaos, 2000: Proceedings of the Second International Conference, edited by F. L. Chernousk and A. L. Fradkov (IEEE, New York, 2000), Vol. 3, p. 552.
[32] V. O. Afenchenko *et al.*, Phys. Fluids **10**, 390 (1998).
[33] J. M. Vega *et al.*, J. Fluid Mech. **372**, 213 (1998).
[34] R. R. Aliev and V. N. Biktashev, J. Phys. Chem. **98**, 9676 (1994).